IDENTIFICATION AND COMPENSATION OF BETATRONIC RESONANCES IN THE PROTON SYNCHROTRON BOOSTER AT 160 MEV

A. Santamaría García [*,1], F. Antoniou[1], S. Albright[1], F. Asvesta[1,2], H. Bartosik[1], G.P. Di Giovanni[1], B. Mikulec[1], H. Rafique[1], [1]CERN, Geneva, Switzerland, [2]NTUA, Athens, Greece

Abstract

The Proton Synchrotron Booster (PSB) is the first circular accelerator in the injector chain to the Large Hadron Collider (LHC) and accelerates protons from 50 MeV to 1.4 GeV. The PSB will need to deliver two times the current brightness after the LHC Injectors Upgrade (LIU) in order to meet the High Luminosity LHC (HL-LHC) beam requirements. At the current injection energy a large incoherent space charge tune spread limits the brightness of the beams, which is one of the main motivations to increase the injection energy to 160 MeV with the injection provided by Linac4, a new H^- linear accelerator. The higher injection energy will allow doubling the beam intensity while maintaining a space charge tune spread similar to current values. The degradation of the beam brightness due to the tune spread can be minimized with a proper choice of working point and an efficient compensation of resonances. In this paper, we present the measurement of the betatronic resonances in the four rings of the PSB at 160 MeV before the Long Shutdown 2, as well as the results of a proposed compensation scheme.

INTRODUCTION

Injection into the Proton Synchrotron Booster (PSB) at CERN is dominated by incoherent space charge effects. Due to the large tune spread at injection energy, which can go up to $\Delta Q = 0.5$ [1], the tune is set far away from the integer resonances, then moves quickly to a resonance-free region as the tune spread shrinks due to acceleration.
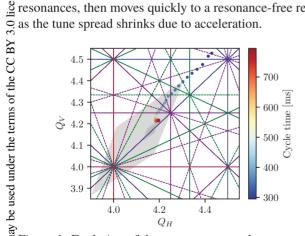

Figure 1: Evolution of the average tune and tune spread in the PSB for the BCMS beam, a low intensity ($\approx 80 \times 10^{10}$) ppb cycle accelerated in a single harmonic RF bucket.

During this process several resonances are crossed, the most important being the half-integer resonance $2Q_V = 9$.

---

* andrea.santamaria@cern.ch

Figure 1 illustrates the change in $Q_{H,V}$ and $\Delta Q_{H,V}$ of the Batch Compression Merging and Splitting (BCMS) cycle [2], used as the main operational LHC filling cycle during 2018. The resonant tune lines are shown up to 4th order, where 1st order resonances are plotted in red, 2nd order in blue, 3rd order in green, and 4th in purple. Skew resonances are shown as dashed lines and normal resonances as solid ones. The tune spread at injection (larger lozenge) and before extraction (smaller lozenge) are also shown [3].

The dynamic resonance crossing of the operational tune can cause both emittance growth and beam loss. Therefore, efficient resonance compensation is key to achieve maximum brightness. A resonance measurement and compensation campaign was carried out at the new injection energy of 160 MeV so that it could serve as comparison for the start of Run 3.

RESONANCE MEASUREMENTS

Measurement Set-Up

A dedicated 160 MeV flat-top cycle was used to perform the resonance measurements at constant energy (shown in Figure 2).
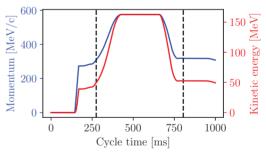

Figure 2: The 160 MeV flat-top energy cycle. The dashed lines indicate injection and extraction times (at 275 ms and 805 ms, respectively).

The beam intensity was recorded with the Beam Current Transformers (BCTs) in the rings and the tune was measured with the BaseBand tune measurement system (BBQ) [4]. The BBQ system kicks the beam transversely and its oscillations are observed at a position pick-up turn by turn. The fractional part of the betatron tune is then extracted by analyzing the frequency components of the amplitude data obtained by the BBQ system. The newly developed Py-NAFF [5] Python library was used for this purpose, which implements the Numerical Analysis of Fundamental Frequencies method [6]. In order to disentangle space charge from machine imperfection effects the beam emittance was

blown-up at the beginning of each cycle to reduce the space charge tune spread. The blow-up was achieved by setting the working point close to an integer resonance. To further limit space charge effects the beam intensity was kept below 160×10^{10} protons and the RF was operated with harmonics 1+2 in bunch lengthening mode, which reduces the peak line density. The measurements were taken at an almost natural chromaticity of $\xi_x = -0.9$ and $\xi_y = -1.4$, with a residual current of -10 A applied to the sextupole family used for chromaticity correction and referred to as XNOH0.

Static Tune Scans

A static tune scan is performed by measuring the amount of lost beam when operating at a specific working point. The tune step for the measurements, determined by the precision of the instruments, was 0.01. This translated into ~ 2000 measurements, which took approximately 20 hours of beam time for each of the four PSB rings. The beam characteristics before measurement are listed in Table 1, and the result of the static tune scans are shown in Fig. 3.

Table 1: Initial Parameters for the Static Tune Scans

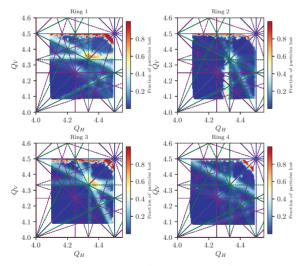|	R1	R2	R3	R4
Bunch Intensity [10^{10} protons]	100	120	130	130
Horizontal emittance [µm.rad]	9.2	7.9	5.9	8.7
Vertical emittance [µm.rad]	8.0	7.8	5.6	8.0
Bunch length [ns]	594	602	577	600
Momentum spread [10^{-3}]	1.28	1.33	1.20	1.33
Space charge tune spread ΔQ_x	0.049	0.065	0.098	0.065
Space charge tune spread ΔQ_y	0.055	0.068	0.11	0.071

Figure 3: Static tune scans for each ring of the PSB with multipoles off, where the tune values are the measured ones.

From Fig. 3 it can be seen that the majority of beam loss occurred at third order resonances, and differed from ring to ring. Crossing the half-integer resonance $2Q_V = 9$ caused total beam loss, which can be seen as the red regions in Fig. 3. The transverse feedback (TFB) was active for all cases except for Ring 2. In this ring it interacted destructively with the beam at certain working points causing losses

unrelated to the resonances. Due to the absence of the TFB an instability developed in Ring 2, which can be observed next to the $3Q_H = 13$ resonant line. On the other hand, some discrepancies were observed between the programmed and measured tune of $\Delta Q_{H,V} \in [-10^{-2}, -10^{-3}]$, which could be explained by a coherent tune shift from impedance [7].

Dynamic Tune Scans

A dynamic tune scan consists of measuring the beam losses while one tune is constant and the other varies linearly with time, scanning all the relevant tune values. This method is orders of magnitude faster than the static tune scan, but as the intensity decreases when crossing resonances early in the scan there may not be sufficient intensity to observe resonances towards the end. To try and ensure all resonances are seen the scans are run from high-to-low and low-to-high tunes, with both Q_H and Q_V as the variable.

The beam parameters listed in Table 2 were used for a scan with Q_V varying from minimum to maximum value while keeping Q_H constant, the results are shown in Fig. 4. We can observe that in this case the resonances are the same as the ones that were identified with the static tune scans, with the difference that we can now observe the coupling line $Q_H = Q_V$ and excluding the instability in Ring 2.

Table 2: Initial Parameters for the Dynamic Tune Scans

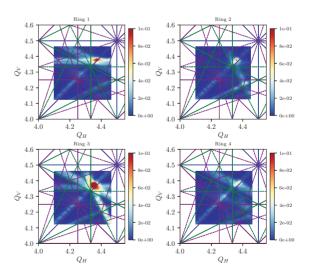|	R1	R2	R3	R4
Bunch Intensity [10^{10} protons]	157	116	131	134
Horizontal emittance [µm.rad]	6.4	7.0	6.1	6.0
Vertical emittance [µm.rad]	8.0	10.6	8.7	7.8
Bunch length [ns]	634	610	610	619
Momentum spread [10^{-3}]	1.43	1.36	1.39	1.39
Space charge tune spread ΔQ_x	0.092	0.062	0.081	0.085
Space charge tune spread ΔQ_y	0.087	0.053	0.072	0.078

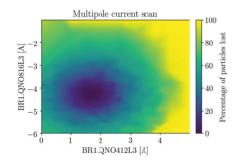Figure 4: Dynamic tune scans for each ring of the PSB.

RESONANCE COMPENSATION

The resonances that are naturally excited in the PSB can be compensated using the available multipole corrector magnets [8]. The PSB is equipped with a variety of corrector

Table 3: Currents of Magnet Correctors for Resonance Compensation Given in Ampères

	$2Q_y = 9$	$Q_x + 2Q_y = 13$	$2Q_x + Q_y = 13$	$3Q_y = 13$	$3Q_x = 13$
Ring 1	BR1.QNO816L3 = -4.33 BR1.QNO412L3 = 1.55	BR1.XNO9L1 = -9.99 BR1.XNO4L1 = -6.07		BR1.XSK6L4 = 2.77 BR1.XSK2L4 = -8.33	
Ring 2	BR2.QNO816L3 = -5 BR2.QNO412L3 = 1.44		BR2.XSK6L4 = -1.42 BR2.XSK2L4 = 4.28		
Ring 3	BR3.QNO816L3 = -3.65 BR3.QNO412L3 = 1.42	BR3.XNO4L1 = 3.15 BR3.XNO9L1 = -24.73	BR3.XSK2L4 = -9.99 BR3.XSK6L4 = 6.66	BR3.XSK2L4 = -0.26 BR3.XSK6L4 = 4.47	BR3.XNO9L1 = -17.14 BR3.XNO4L1 = 4.28
Ring 4	BR4.QNO816L3 = -3.83 BR4.QNO412L3 = 2.94	BR4.XNO9L1 = -8.68 BR4.XNO4L1 = 7.63			

magnets such as normal and skew quadrupoles, normal and skew sextupoles, and normal and skew octupoles. The Resonance Driving Terms (RDT) for each corrector were calculated in terms of amplitude and phase using PTC [9] in MAD-X [10]. Corrector pairs with orthogonal orientation of their driving term in the RDT space were chosen, as this allows compensating any orientation of the machine residual RDT [11, 12]. Once the most suitable pair is identified, the optimal current configuration can be determined experimentally. To this end, a specific resonance is selected and crossed dynamically as described in the previous section for a variety of current configurations of the corrector pair. The intensity is monitored before and after the resonance crossing and the losses resulting from the resonance are identified. The current configuration resulting in the lowest losses is the one that will best compensate the resonance. This is illustrated in Fig. 5, which shows a current scan performed to compensate resonance $2Q_y = 9$ in Ring 1. The region of lowest losses can be clearly identified.

Figure 5: Current scan of a pair of normal quadrupole families.

Following the same procedure for all the measured resonances we arrive to a full compensation scheme, shown in Fig. 6. We can observe that the operational tune space is clear, and that the $2Q_y = 9$ has been considerably reduced and can now be crossed. We can see the excitation of the $3Q_y = 13$ resonance in Ring 3 since not all resonances could be compensated simultaneously due to the number of available corrector sextupoles. An alternative compensation scheme exists for this case, where the $2Q_x + Q_y = 13$ resonance would be excited instead. Table 3 summarizes the specific current values used for compensation.

The proposed compensation scheme was applied to the highest intensity beam produced in the PSB, of an average 950×10^{10} ppr, with the current scaled to the beam rigidity
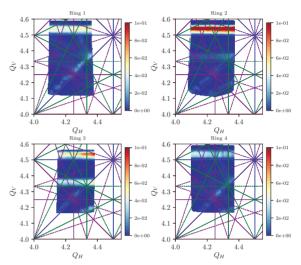

Figure 6: Dynamic tune scans for each ring of the PSB with the proposed compensation scheme.

along the full cycle. The beam could be accelerated as done before in operation, confirming the effectiveness of the new corrections.

CONCLUSIONS

The betatronic resonances present in the PSB at the end of Run 2 were measured with two different methods. Third order resonances were present in all rings, although they differed from ring to ring. The reduction of the strength of the resonances to minimal values was achieved by selecting optimal pairs of magnet correctors and measuring the most efficient current configuration. This study provides a snapshot of the status of the PSB resonances before LS2 and can be used for comparison in Run 3.

ACKNOWLEDGMENTS

REFERENCES

[1] V. Raginel G. Rumolo B. Mikulec, A. Findlay and G. Sterbini. Tune spread studies at injection energies for the CERN Proton Synchrotron Booster. In Proc. of HB2012, Beijing, China, 17-21, Sep. 2012.

[2] H. Bartosik et al. Injectors Beam Performance Evolution during Run 2. 9th LHC Operations Evian Workshop, 2019. `https://indico.cern.ch/event/751857/contributions/3259375/attachments/1820780/2987151/Evian2019_injectors.pdf`.

[3] A. Oeftiger. Space Charge Tune Spread Tool. Space Charge Working Group Meeting February 16, 2017. `http://frs.web.cern.ch/frs/Source/space_charge/Meetings/meeting88_16.02.2017/tunespreadtool.pdf`.

[4] M. Gasior and R. Jones. High sensitivity tune measurement by direct diode detection. In 7th European Workshop on Beam Diagnostics and Instrumentation for Particle Accelerators (DIPAC 2005) Lyon, France, June 6-8, 2005, pages 310–312, 2005.

[5] N. Karastathis, F. Asvesta, and P. Zisopoulos. `https://pypi.org/project/PyNAFF/`.

[6] J. Laskar, C. Froeschlé, and A. Celletti. The measure of chaos by the numerical analysis of the fundamental frequencies. application to the standard mapping. Physica D: Nonlinear Phenomena, 56(2):253 – 269, 1992.

[7] C. Zannini, G. Iadarola, B. Jones, K. Li, T. Rijoff, and G. Rumolo. Transverse Impedance Model of the CERN-PSB. (CERN-ACC-2015-334):MOPJE050.3 p, 2015.

[8] P. Urschütz. Measurement and compensation of second and third order resonances at the CERN PS Booster. In 9th European Particle Accelerator Conference (EPAC 2004) Lucerne, Switzerland, July 5-9, 2004, 2004.

[9] F. Schmidt, E. Forest, and E. McIntosh. Introduction to the polymorphic tracking code: Fibre bundles, polymorphic Taylor types and "Exact tracking". Technical Report CERN-SL-2002-044-AP. KEK-REPORT-2002-3, CERN, Geneva, Jul 2002.

[10] L. Deniau. `http://madx.web.cern.ch/madx/`.

[11] F. Asvesta, H. Bartosik, A. Huschauer, Y. Papaphilippou, and G. Sterbini. Resonance identification studies at the CERN PS. Journal of Physics: Conference Series, 1067:062021, Sep 2018.

[12] F. Asvesta, F. Antoniou H. Bartosik, G. P. Di Giovanni, and Y. Papaphilippou. Coupling and Space Charge Studies at the CERN PSB, presented at the 10th Int. Particle Accelerator Conf. (IPAC'19), Melbourne, Australia, May 2019, paper WEPTS041, this conference.